Acoustic Properties of Lightweight Micro-Perforated Plate Systems

Thomas Dupont, Goran Pavić, Bernard Laulagnet

Acoustic Properties of Lightweight Micro-Perforated Plate Systems

T. Dupont, G. Pavic, B. Laulagnet
Laboratoire Vibrations-Acoustique, INSA de Lyon, 25 bis, avenue Jean Capelle, 69621 Villeurbanne, France

Summary
The paper extends the investigation of micro-perforated plates, originally initiated by Maa, into acoustic prop-erties by considering the coupling of such a plate with an ordinary flexible plate through an air gap. It has been found that the resulting two plate system, with one of the plates being micro-perforated, can provide potentially interesting performance while still remaining free of any classical absorption material. The analysis is limited to infinite plates, with the consideration of the cases of normal, oblique and diffuse incidence. A classical wave approach is used to model the absorption and the transmission of a micro-perforated plate backed by a simple plate. Formulae are supported by plots which illustrate the system performance in potentially applicative cases. Measurements done in the Kundt tube and in an experimental window have confirmed the validity of the devel-oped model. By acting on the parameters of the system, i.e. the perforation rate, hole diameter, gap width and plate thickness, the absorption and transmission coefficients of the system can be tuned, within certain limits, for increased efficiency in a selected frequency range. The presence of a second flexible plate was shown to increase transmission loss, reduce the reflection effect and weaken the coincidence effect.

1. Introduction

Sound transmission and reflection by panels has been a topic widely addressed in the past, with the pioneering studies originating already from the 1930's. An exact solution of sound transmission through a plane solid layer, applicable to both thin and thick plates, was given in [1]. Investigations on the transmission through single panels, see e.g. [2, 3], were extended to double walls and more complex systems [4, 5, 6, 7, 8, 9, 10].

One of the original ideas was that of Maa [11, 12, 13] who investigated absorption of micro-perforated panels (MPP) coupled to a rigid wall. Contrary to an ordinary panel resonator, which needs an additional absorption layer to be effective, a MPP backed by a wall has the advantage of combining resonant and absorption effects. Moreover, the absence of classical absorption material, which potentially presents a risk of pollution and sometimes even a fire hazard, makes a MPP a "clean" design solution of superior aesthetic and hygienic properties. MPP-based solutions could be used in the transport industry, civil engineering, and in acoustic panel design. Such designs have already been proposed [14, 15, 16, 17].

This paper deals with the transparency and absorption of a MPP coupled to a thin plate. To the best of the authors' knowledge such a combination has never been investigated before. The system MPP–thin plate is radically different from the system MPP–hard wall, both in the physics of sound transmission and in the areas of potential applicability. While the latter is meant to provide absorption to rooms and enclosures, the former is supposed to act as a lightweight sound barrier which, if successfully optimised, can provide improved combined properties of absorption, reflection and transmission.

2. Sound propagation at normal incidence

2.1. Model of MPP backed by resonant loading

This section considers plane wave propagation normal to the surface of the micro-perforated plate (MPP) which is taken to be infinite. The MPP is backed by a solid plate, placed in parallel at some distance away, Figure 1. As the incidence is normal, the solid plate is represented as a single degree-of-freedom mass-spring-dashpot system. This configuration is chosen to analyse the effect of MPP backing by a single resonant mechanical mode which could be one of the modes of an otherwise complex multi-modal system. Some preliminary results using such a model were reported in [18].

The principle upon which a MPP operates is the thermo-viscous effect. When the sound wave enters the perforation, the air viscosity converts one part of acoustic energy into heat. A portion of this heat is taken away by the MPP itself. The viscous forces in the perforation depend on the radial gradient of sound particle velocity. The axial velocity is zero on the boundary, increases abruptly across the

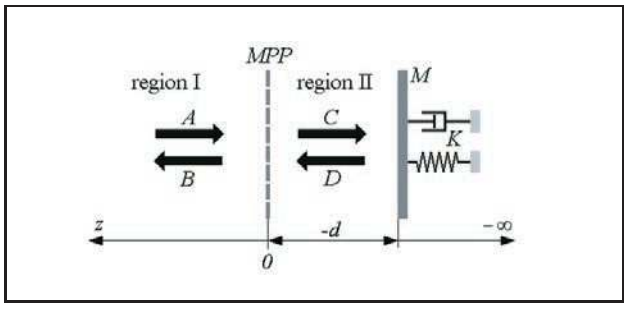

Figure 1. Scheme of MPP backed by resonant loading. A, B, C, D are the pressure amplitudes, K and M are the stiffness and mass of the load.

boundary layer and becomes nearly constant in the interior of the perforation hole.

The thickness of the boundary layer depends on kinematic viscosity ν, $d_v \propto \sqrt{\nu}$. In the boundary layer region the viscous acoustic model, based on Kirchhoff's equation, describes the axial velocity profile in terms of Bessel functions. This model fails if the perforation diameter is too large. Maa considers the model valid up to the frequency which corresponds to the first acoustic transversal mode of perforation.

To take into account heat conduction in the MPP's sheet material, an added viscous term was introduced by Crandall [19] and improved by Melling [20]. The kinematic viscosity of air $\nu_0 = 1.56 \cdot 10^{-5}\,\mathrm{m^2/s}$ is added by a correction term $2 \cdot 10^{-5}\,\mathrm{m^2/s}$. Maa [11] has shown that the correction was not needed when the MPP's thickness was lower than the perforation diameter.

Using the results by Crandall [19], Maa [11] has worked out the normal acoustic impedance of very small tubes. This result was later generalised to micro-perforated plates as follows: if the perforations do not mutually interfere, implying the hole diameter is several times smaller than the distance between holes, the specific acoustic impedance of a MPP becomes equal to the specific acoustic impedance of a single perforation divided by the perforation rate of the plate p equal to the ratio perforated area / plate area.

Maa's model neglects the influence of MPP vibration on sound absorption. In addition, it neglects the part of sound reflected by the solid part of the MPP, providing the distance between the holes is small compared to wavelength.

The viscous effect becomes significant in the case of very small perforations; the diameter should be comparable to the thickness of the boundary layer. Thus submillimetre perforation diameters are needed to make the viscous effect work in air. If, however, the diameter becomes overly small, the absorption decreases again as the motion of the air gets blocked.

The MPP model assumes the existence of particle velocity continuity at the two sides of MPP. If the plate thickness is very small, an interaction may occur between viscous effects and plate vibration. If the thickness gets large, the hypothesis of the velocity continuity on the two plate faces becomes invalid. The thickness thus has to remain small compared to the wavelength to ensure the model validity.

In the case of normal incidence, the MPP specific impedance reads, [11]:

$$z_{mpp} = y + \mathrm{j}\omega m, \tag{1}$$

$$m = \frac{t}{\rho c}\left(1 + \frac{1}{\sqrt{3^2 + x^2/2}} + 0.85\frac{a}{t}\right), \tag{1a}$$

$$y = \frac{32\nu t}{\rho c a^2}\left(\sqrt{1 + \frac{x^2}{32}} + \frac{\sqrt{2}ax}{8t}\right), \tag{1b}$$

with $$x = \sqrt{\frac{\omega}{\nu}}\frac{a}{2}. \tag{1c}$$

Here m and y are the normalised specific mass and resistance of the MPP respectively, t its thickness (m), a the hole diameter (m), ω the radian frequency, while ν, ρ and c are the kinematic viscosity, the fluid mass density and the fluid sound speed, respectively.

The absolute (non-normalized) impedance reads:

$$Z_{mpp} = z_{mpp}\rho c. \tag{2}$$

The region in front of the MPP is supposed infinite, thus the incident waves are unaffected by the waves reflected from the MPP into this region. Excitation is supposed harmonic, taken into account by the frequency multiplier $\mathrm{e}^{\,\mathrm{j}\omega t}$ which will be omitted in the rest of the paper.

The pressure amplitudes read (the upper case symbols denote complex amplitudes):

region I: $$P_I(z) = A\mathrm{e}^{\mathrm{j}kz} + B\mathrm{e}^{-\mathrm{j}kz}, \tag{3a}$$

region II: $$P_{II}(z) = C\mathrm{e}^{\mathrm{j}kz} + D\mathrm{e}^{-\mathrm{j}kz}. \tag{3b}$$

The boundary conditions are:

- At $z = 0$, the particle velocity continuity applies: $v_I(z = 0^-, t) = v_{II}(z = 0^+, t)$. The MPP impedance equals the net pressure acting on the MPP divided by the particle velocity:

$$Z_{mpp} = \left.\frac{P_{II} - P_I}{V}\right|_{z=0}. \tag{4}$$

- At $z = -d$, the particle velocity continuity implies: $v_{II}(z = -d^-) = \mathrm{j}\omega w$ where $w = W\mathrm{e}^{\mathrm{j}\omega t}$ is the displacement of the backing plate. The unit-area force balance at this boundary reads:

$$KW - \omega^2 MW = P_{II} - \mathrm{j}\omega\rho cW, \tag{5}$$

where M and K are the unit mass and unit stiffness, respectively. The damping is accounted for by making K complex. The term $\mathrm{j}\omega\rho cW$ represents the complex amplitude of air pressure applied to the back of the solid plate, region III, due to acoustical radiation loading. This term will be added to the imaginary part of K which represents structural damping.

The power balance has to be satisfied at the MPP surface:

$$I_{inc} = I_{ref} + I_{load} + I_{mpp}, \tag{6}$$

where I_{inc}, I_{ref}, I_{load} and I_{mpp} are the net (i.e. time averaged) intensities of incident wave, reflected wave, intensity absorbed by the load, and intensity absorbed by the MPP.

In general, the net intensity is (overbar stands for complex conjugate):

$$I = \frac{1}{2}\Re e\{P\overline{V}\}.$$

The intensities absorbed by the MPP and the load read:

$$I_{mpp} = \frac{1}{2}\left|V_{z=0}\right|^2 \Re e\{Z_{mpp}\}, \tag{7a}$$

$$I_{load} = \frac{1}{2}\left|V_{z=d}\right|^2 \Re e\{Z_{load}\}, \tag{7b}$$

with the load impedance:

$$Z_{load} = \frac{K - M\omega^2}{\mathrm{j}\omega}. \tag{7c}$$

Dividing (6) by I_{inc} the equilibrium of energy coefficients is obtained:

$$1 = r + \alpha, \qquad \alpha = \alpha_{mpp} + \alpha_{load}, \tag{8}$$

with $\alpha_{load} = \alpha_\varepsilon + \tau$, where r, α and τ are the coefficients of reflection, transmission (included in load absorption) and absorption due to the MPP.

The resolution of governing equations under the given boundary conditions gives:

$$r = \frac{\left|z_{mpp}/2\big(1 - \mathrm{e}^{-2\mathrm{j}kd}\beta(\omega)\big) + \mathrm{e}^{-2\mathrm{j}kd}\beta(\omega)\right|^2}{\left|z_{mpp}/2\big(1 - \mathrm{e}^{-2\mathrm{j}kd}\beta(\omega)\big) + 1\right|^2}, \tag{9}$$

$$\alpha_{mpp} = \frac{I_{mpp}}{I_{inc}} = \frac{\frac{1}{2}\big(1 - \beta\mathrm{e}^{-\mathrm{j}kd}\big)\Re e\{z_{mpp}\}}{\left|z_{mpp}/2\big(1 - \mathrm{e}^{-2\mathrm{j}kd}\beta\big) + 1\right|^2}, \tag{10}$$

$$\alpha = \frac{I_{mpp} + I_{load}}{I_{inc}} = 1 - r, \tag{11}$$

$$\text{with} \quad \beta = \frac{(K - M\omega^2) - \mathrm{j}\omega\rho c}{(K - M\omega^2) + \mathrm{j}\omega\rho c}. \tag{12}$$

Several numerical simulations were done at this point using the following parameters:

- MPP: steel, thickness 1.5 mm, perforation 3% (circular holes).
- load: mass density 78 kg/m^2 (corresponding to a steel sheet of 10 mm thickness), unit stiffness: $K = 3.08 \cdot 10^8$ N/m^3, internal plate loss factor 10^{-2}, radiation resistance $\omega\rho c/K$.
- air gap: 0.15 m.

Figure 2 shows the absorption of the double plate system analysed. For the sake of comparison, the absorption of a similar system having the solid plate blocked (i.e. rigid wall) is shown too.

A fully rigid load would minimise absorption at frequencies where the gap width is a multiple of half the wavelength, $d = n\lambda/2$, n - integer. At these frequencies the sound velocity on the MPP drops to zero; the viscous effect thus vanishes.

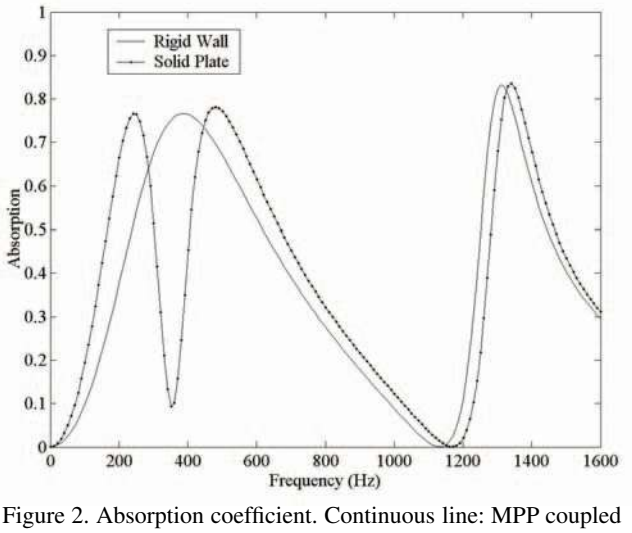

Figure 2. Absorption coefficient. Continuous line: MPP coupled to a rigid wall; dotted line: MPP coupled to a plate (steel, thickness 10 mm, spring rate / unit area: $K = 3.08 \cdot 10^8$ N/m, internal loss factor = 10^{-2}). MPP: steel, thickness $t = 1.5$ mm, perforation rate 3%, circular holes diameter $a = 0.5$ mm. Cavity gap is $d = 0.15$ m.

However, the maximum of absorption does not correspond to frequencies where the gap width is $d = (2n + 1)\lambda/4$ which is the condition of maximum particle velocity at the MPP surface. When the sound enters perforations a plate reaction occurs which affects absorption. This is taken into account by adding a mass to the MPP impedance (imaginary part of Z_{mpp}). The maximum occurs at $\cot(kd) = \omega\Im m\{Z_{mpp}\}$ and not at $\cot(kd) = 0$ making thus the maximum absorption shift to lower frequencies, the shift being larger the higher the frequency.

The particle velocity at the load surface is not zero. The resonance effect due to the load can be seen near 350 Hz as a sharp dip, which is a consequence of load impedance drop. Far from this frequency, the difference in absorption between the cases of resonant load and rigid wall is negligible, as the surface velocity of the load drops in this region virtually to zero. The contribution to absorption of the MPP, represented by a dash-dot line, is seen to represent the dominant mechanism of the overall absorption, even at load resonance.

For each particular configuration the absorption can be optimised by adjusting the system parameters. The maximum absorption which can be attained this way can be fairly high in certain frequency bands. The main effect in the overall absorption is the viscous effect, the damped resonance effect of the backing cavity being of lesser importance. It could thus be expected that the overall absorption would be further increased by increasing the kinematic viscosity inside the perforations.

Two simple methods were attempted to increase the absorption by increasing viscosity: the first one consists in

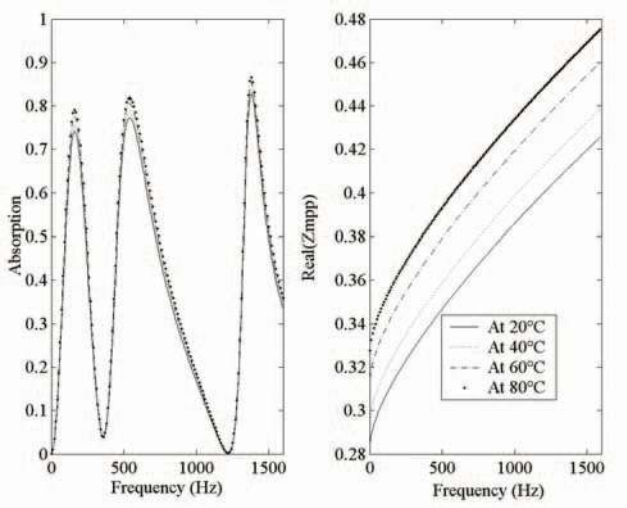

Figure 3. Absorption coefficient of the two plate system and real part of MPP acoustic impedance computed for different air temperatures. The MPP characteristics are: steel, thickness $t = 1.5$ mm, perforation rate 3%, hole diameter $a = 0.5$ mm, cavity gap $d = 0.15$ m. Backing plate: steel, thickness 10 mm. Spring rate per unit area: $K = 3.08 \cdot 10^8$ N/m, internal loss factor = 10^{-2}.

Table I. Properties of fluids relative to viscous sound absorption.

	viscosity [m^2/s]	mass density [kg/m^3]	speed of sound [m/s]
air	$1.5 \cdot 10^{-5}$	1.29	340
water	$1.013 \cdot 10^{-6}$	1000	1500
glycerine	$6.8 \cdot 10^{-4}$	1264	1920

heating the MPP, the second one to replace the air in the MPP holes by a more viscous fluid, like oil.

The rise of kinematic viscosity with temperature is given by Sutherland's formula, [21]:

$$\nu = \frac{\mu}{\rho} = \nu_0 \sqrt{\frac{T}{243}} \frac{1 + S_{243}}{1 + S_T}, \tag{13}$$

with T = absolute temperature (°K), $S = 110.4$°K, $\nu_0 = 1.711 \cdot 10^{-5}$ m^2/s for air.

Heating the plate results in an increase of perforation diameter. This effect was computed to be negligible for not too high temperatures and was thus disregarded.

Figure 3, left, shows the computed influence of heating an MPP on system absorption for a range of temperatures. Figure 3, right, shows the real part of MPP normalised impedance at the same temperatures. While the increase in the real part of impedance with temperature is significant, the increase in overall absorption is fairly small. Thus the conclusion that heating the MPP would not be an efficient way to improve its sound absorption.

The second method, i.e. adding viscous material to a MPP, was readily realised because a MPP keeps viscous fluid imprisoned in the holes. Several experiments were carried out in a Kundt tube using two different filling fluids, water and glycerine. The properties of these fluids are compared to the properties of air in Table I.

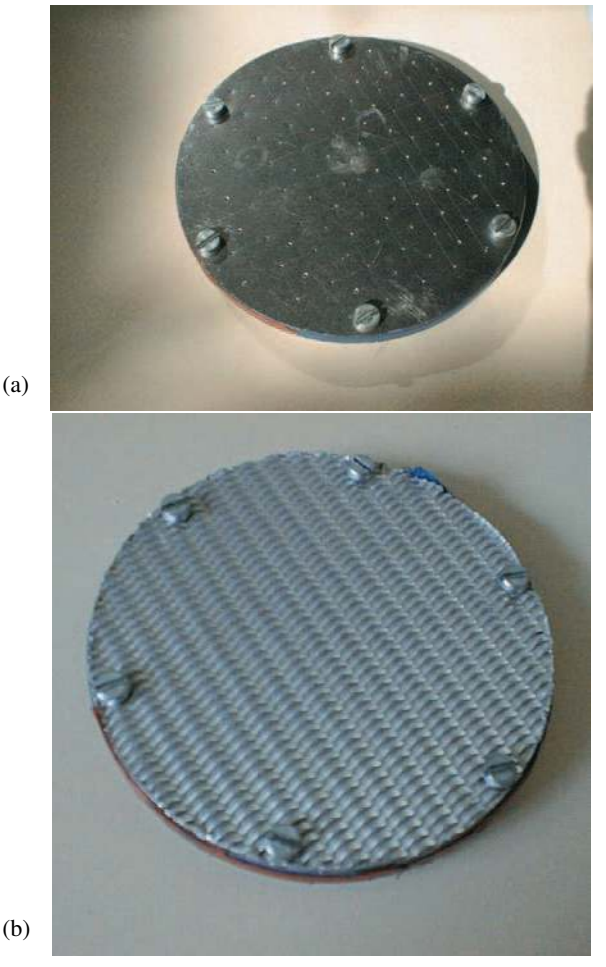

Figure 4. Photos of two MPP Kundt tube samples : a) hand made steel plate, thickness 1 mm perforated with circular holes of 0.5 mm diameter and 0.55% perforation ratio. b) industrial dural plate, thickness variable between 1 and 1.7 mm, slit perforations of 0.4 mm equivalent diameter and 3.5% perforation ratio.

It was found that in spite of $\nu_{\mathrm{glycerine}} > \nu_{\mathrm{air}} > \nu_{\mathrm{water}}$ the absorption effect of adding heavy fluids was very weak. Water and glycerine have a mass density much larger than air. This mass is responsible for a screening effect acting on the perforations, which causes increased sound reflection of the MPP. Thus replacing the air in perforations with viscous liquid actually destroys the acoustic absorption performance of the system. Several experiments carried out in a Kundt tube well confirmed this conclusion which in turn implies that a MPP system could not be used in open spaces because of humidity and rain which could make it lose good absorption properties.

2.2. Experimental part: measurement in the Kundt tube

To check the validity of the MPP model, a B&K Kundt tube was used to measure the acoustical characteristics of a MPP coupled to a rigid termination across an air gap. The frequency range was chosen between 0 and 1600 Hz

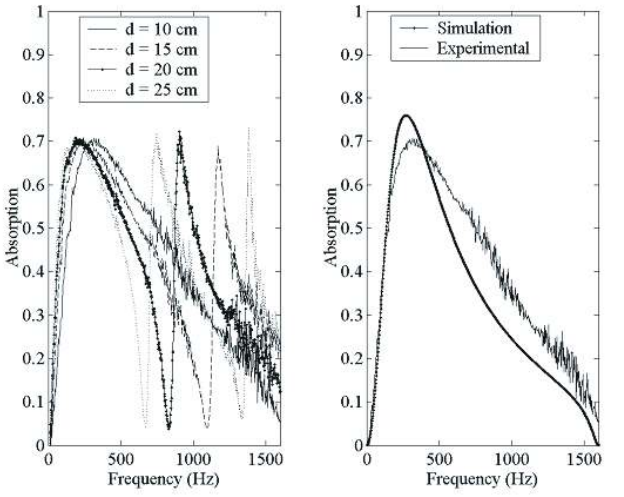

Figure 5. Absorption coefficient of a MPP coupled to a rigid wall: custom made steel plate, thickness 1 mm, circular holes of 0.5 mm diameter and 0.55% perforation ratio. Experimental results for different cavity gaps: 0.10, 0.15, 0.20, 0.25 m, (left); comparison between simulation and experimental results for a 0.1 m gap (right).

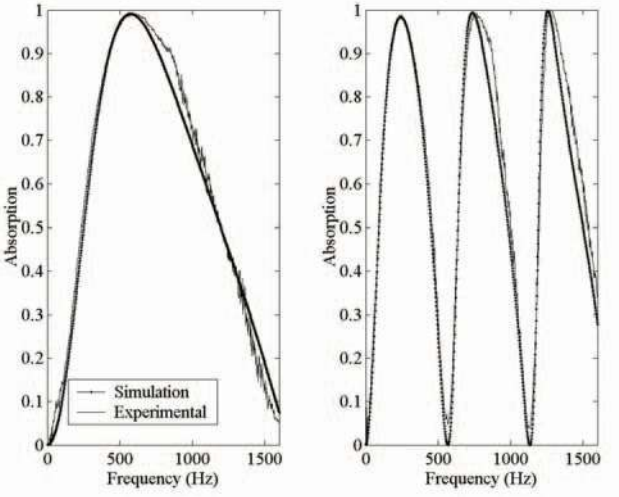

Figure 6. Comparison of computed and experimental absorption coefficient of a MPP (industrial plate, dural, thickness 1–1.7 mm, slit perforation $a_{eq} = 0.4$ mm, $p = 3.5\%$, louvre structure) coupled to a rigid wall at two cavity gaps: $d = 0.1$ m (left) and $d = 0.3$ m (right).

to make sure only plane waves existed in the tube. The existence of plane waves corresponds closely to the analysed case of normal incidence. These results were then compared to the theoretical ones obtained by computation.

An aluminium support was made to hold the MPP in place by small screws located at its circumference. Two different MPPs were tested, Figure 4:

- a custom-made steel plate of 1mm thickness with circular perforations of 0.5 mm radius and the perforation rate of 0.55%.
- an industrial MPP produced by Sontech (Sweden). This plate was made in dural with a louvre structure and slit perforations. The plate thickness was found to vary from 1 mm to 1.7 mm. The slit was modelled in computations as an equivalent circular hole of the same area. This has produced the hole radius of 0.4 mm. The percentage perforation was 3.5%.

The purpose of using the custom-made MPP was to bring the simulation as close to experiments as possible. Its characteristics as defined by the model, i.e. the hole diameter, the percentage perforation and the thickness were easy to identify directly. The industrial MPP was used to check the applicability of the developed model to real cases where the geometry could not be identified in a straightforward way (slit-shaped holes, rugged surface).

Figure 5, left, shows the measurement results taken on a custom-made MPP at 4 air gap values. It can be seen that the frequencies of maximum absorption as well as absorption bandwidths change with the gap width d. The number of maxima increases with d as expected, while the effective absorption bandwidth decreases with d. However, the maximum absorption value remains unaffected, around 0.7. One can note good absorption of the MPP system at 50–300 Hz. A typical porous material could not absorb any better at these low frequencies.

A comparison between model computation and experiments for the custom MPP is shown on Figure 5, right. One can notice that the matching between theory and experiment is globally good, although the model predicts an absorption peak of smaller band width and higher maximum than the experiment showed. However, both curves display a similar shape. Heat created by the motion of air in the perforation will be transferred to the support. This loss has to be taken into account, which was done by increasing the viscosity coefficient as defined in [11].

Figure 6 shows experimental and computed results obtained on the Sontech MPP coupled to a rigid wall via a 0.1 m air gap. As the true characteristics of this MPP were not fully known (perforation geometry and surface being irregular), iterations were made until the best fit of measurement results was achieved. The equivalent parameters were found to be: thickness - 1.25 mm, equivalent diameter of circular perforation - 0.4 mm, perforation rate 3.5%. Using these parameters, the experiment matched the computation well.

Once the plate parameters were identified, the measurements were repeated using a larger air gap, 0.3 m. The Sontech MPP was found to have a very good absorption at low and medium high frequencies.

The increase in the absorption of Sontech's MPP is attributed to the form of the hole (slit), which has a larger circumference-to-area ratio than circular holes of the custom-built MPP. The increase of this ratio increases the viscous effect as the friction surface increases while the effective diameter drops. Better absorption of Sontech's MPP is also due to a higher perforation percentage and the use of a louvre structure chosen to increase friction. It could be assumed that star-shaped holes may further increase friction and thus improve the MPP performance.

3. Sound propagation at oblique incidence

3.1. Governing equations

The system considered consists of one MPP and one ordinary plate of thickness t_1 and t_2 respectively, Figure 7. The regions I and II are supposed infinite; the same applies to the size of two plates.

An acoustical plane wave is assumed to impinge the MPP at oblique incidence. The selected symmetry of the coordinate system with the wave front makes the case two-dimensional.

The pressure and normal particle velocity amplitudes in the three regions read:

region I:
$$P_I(x,z) = P_{inc}(x,z) + P_{ref}(x,z) = \mathrm{e}^{-\mathrm{j}k_x x}\Big(A\mathrm{e}^{\mathrm{j}k_z z} + B\mathrm{e}^{-\mathrm{j}k_z z}\Big), \quad (14a)$$
$$V_{Iz}(x,z) = \frac{\mathrm{e}^{-\mathrm{j}k_x x}\cos\theta}{\rho_0 c}\Big(B\mathrm{e}^{-\mathrm{j}k_z z} - A\mathrm{e}^{\mathrm{j}k_z z}\Big), \quad (14b)$$

region II:
$$P_{II}(x,z) = \mathrm{e}^{-\mathrm{j}k_x x}\cos\theta\Big(D\mathrm{e}^{-\mathrm{j}k_z z} + C\mathrm{e}^{\mathrm{j}k_z z}\Big), \quad (14c)$$
$$V_{IIz}(x,z) = \frac{\mathrm{e}^{-\mathrm{j}k_x x}\cos\theta}{\rho_0 c}\Big(D\mathrm{e}^{-\mathrm{j}k_z z} - C\mathrm{e}^{\mathrm{j}k_z z}\Big), \quad (14d)$$

region III:
$$P_{III}(x,z) = E\mathrm{e}^{-\mathrm{j}k_x x}\,\mathrm{e}^{-\mathrm{j}k_z z}, \quad (14e)$$
$$V_{IIIz}(x,z) = -E\frac{\mathrm{e}^{-\mathrm{j}k_x x}\cos\theta}{\rho_0 c}\mathrm{e}^{\mathrm{j}k_z z}, \quad (14f)$$

with $k_x = k\sin\theta$, $k_y = k\cos\theta$ and $k = \omega/c$.

The two plates were supposed to be thin enough to ensure particle velocity continuity on each of their faces. Plate impedance expression (1), §2, applies with V replaced by V_z.

The plates impedances of the MPP is the one from §2, equation (1). The impedance of the solid plate is given by:

$$Z_{sp} = \frac{\omega^2\rho_{sp}t_{sp}}{\mathrm{j}\omega}\Big(\frac{c_{sp}^4\sin^4\theta}{c^4} - 1\Big), \quad (15a)$$

c_{sp} being the bending velocity:

$$c_{sp}^4 = \Big(\frac{Et_{sp}^2}{12(1-\nu^2)\rho_{sp}}\Big)\omega^2, \quad (15b)$$

with ν = Poisson coefficient, E = Young's modulus and ρ_{sp} = plate density.

The above system of equations for pressure amplitudes A, B, C, D, E and the amplitude of solid plate displacement F is resolved in the Appendix. The amplitudes are expressed in terms of the incident amplitude A.

The components of the incident intensity vector are given by:

$$I_x = \frac{\Re e\{P_{inc}\overline{V_{inc,x}}\}}{2}, \quad (16)$$

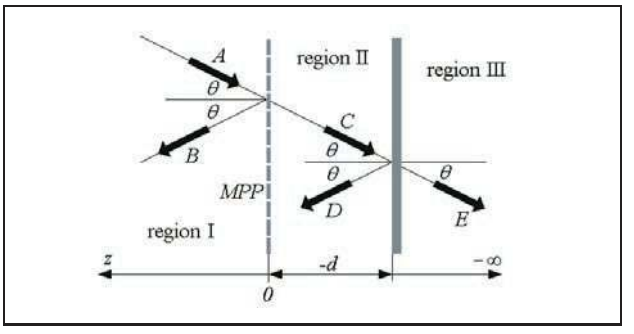

Figure 7. Two-dimensional infinite system in oblique incidence: a MPP plate in tandem with a solid plate separated by an air gap.

$$I_z = \frac{\Re e\{P_{inc}\overline{V_{inc,z}}\}}{2} = \frac{|A|^2}{2\rho_0 c}\cos\theta, \quad (17)$$

with the rest of intensities I_{trans}, I_{ref}, having similar component representation.

Only the normal acoustic velocity v_z is affected by the plate impedance, thus the direction of plate absorption intensity is $\hat{z}$:

$$\vec{I}_{abs\_mpp} = \frac{1}{2}\big|V_z(z=0)\big|^2\Re e\{Z_{mpp}\}\hat{z}$$

and

$$\vec{I}_{abs\_sp} = \frac{1}{2}\big|V_z(z=-d)\big|^2\Re e\{Z_{sp}\}\hat{z}.$$

On the $\hat{z}$ axis an intensity balance applies:

$$|I_{z\_inc}| = |I_{z\_ref}| + |I_{z\_trans}| + |I_{abs\_mpp}| + |I_{abs\_sp}|.$$

The energy coefficients read:

reflection:
$$r(\theta,f) = \left|\frac{I_{z\_ref}}{I_{z\_inc}}\right| = \frac{|B|^2}{|A|^2}, \quad (18a)$$

transmission:
$$\tau(\theta,f) = \left|\frac{I_{z\_trans}}{I_{z\_inc}}\right| = \frac{|E|^2}{|A|^2}, \quad (18b)$$

transmission loss:
$$R(\theta,f) = 10\log_{10}\frac{1}{\tau}, \quad (18c)$$

absorption of MPP:
$$\alpha_{mpp}(\theta,f) = \left|\frac{I_{abs\_mpp}}{I_{z\_inc}}\right|, \quad (18d)$$

absorption of solid plate:
$$\alpha_{sp}(\theta,f) = \left|\frac{I_{abs\_sp}}{I_{z\_inc}}\right|. \quad (18e)$$

3.2. Influence of MPP vibration on sound transmission

In the experiments at normal incidence, §2, an accelerometer was placed on the MPP which has revealed non-negligible plate vibration. The Maa model does not take in account the plate vibration, the plate being supposed fully rigid.

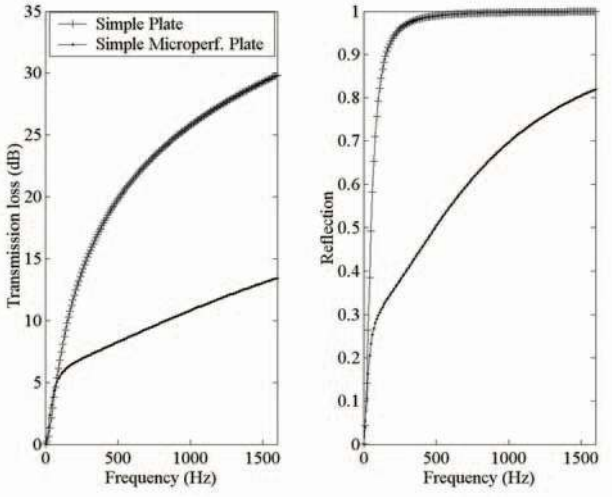

Figure 8. Comparison by computation of absorption (top), transmission loss (left) and reflection coefficient (right) at normal incidence of a single infinite MPP (steel, diameter 0.5 mm, perforation rate 0.55%) and an equivalent unperforated single plate.

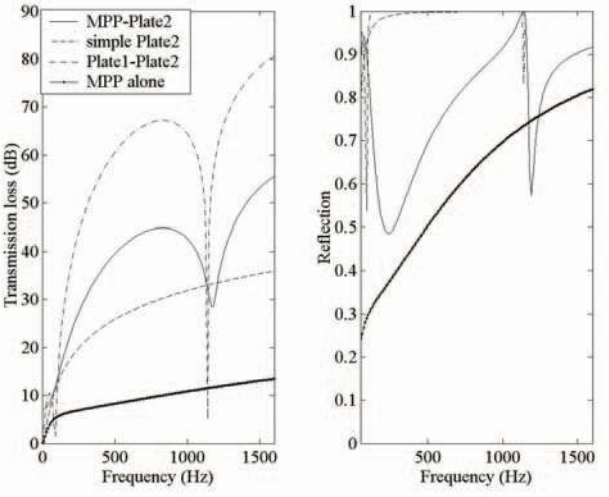

Figure 9. Transmission loss (left) and reflection coefficient (right) computed for normal incidence. The curves represent the basic system (MPP + solid plate), simple plate alone, two simple plates and MPP alone. The MPP's is made of steel, hole diameter 0.5 mm, thickness 1 mm, perforation ratio 0.55%. The steel solid plate is 0.7 mm thick. The air gap is 0.15 m.

The normal motion of a real plate will modify the part of velocity responsible for the viscous effect. If the plate motion is in phase with the acoustic motion, the viscous effect will be reduced, and the plate transparency will be modified too.

If the plate velocity is of the same order of magnitude as the air particle velocity, the MPP impedance could be totally modified. On the other hand, if the plate velocity is negligible with respect to the particle velocity, the MPP impedance as defined in §2 stays valid. In order to take the MPP vibrations into account and to keep the existing MPP impedance model valid, an effective impedance has been formulated combining the classical MPP impedance and MPP vibration. Such a solution has been already used by Kang and Fuchs [16] and applied to an absorption system composed of a micro-perforated membrane coupled to a rigid wall.

The effective MPP impedance is a parallel connection of two constituent impedances:

$$\frac{1}{Z} = \frac{1}{Z_{vib}} + \frac{1}{Z_{mpp}}, \tag{19a}$$

$$Z_{vib} = \frac{\omega^2 \rho_{mpp} t}{\mathrm{j}\omega}\left(\frac{c_{mpp}^4 \sin^4\theta}{c^4} - 1\right) \tag{19b}$$

with MPP bending velocity, c_{mpp}, being of the same form as that of the solid plate, equation (15b).

It has been found using equations (18) that, except at very low frequencies, the plates having the thickness > 0.2 mm will have a vibration impedance much larger than the impedance due to the perforations, $Z_{vib} \gg Z_{mpp}$, thus the conclusion that the MPP vibration can be neglected compared with the viscous effect. The plate vibration will not affect the effective absorption. Moreover, the holes have a tendency to diminish the plate vibrations as the driving acoustic charge applied on the plate drops in the presence of perforations due to fluid circulation.

Figure 8b shows the comparison between the MPP transmission loss due to the viscous effect only and the loss of an equivalent simple plate (i.e. the same plate but without perforations). The difference between the two losses is seen to be very large, exceeding 25 dB at higher frequencies. The viscous model shows well that the MPP transparency is not comparable to that of a solid plate. It can be thus concluded that since the vibration of the solid plate is of the level well below that responsible for the viscous effect, the (even lower) vibration of MPP can be neglected.

3.3. Analysis of transmission and absorption

3.3.1. Transmissibility and absorption of a MPP alone

The viscous effect of a single MPP is maximum at low frequencies, the boundary layer increasing with frequency decreasing, as seen in Figure 8. Between 10 and 350 Hz the MPP absorption exceeds 40%.

The transmission loss of the equivalent solid plate increases by 30 dB from low to medium frequencies, 10→1600 Hz. At these frequencies, the transmission loss of the MPP increases only by one half of this value, i.e. from 0 to 14 dB. This is accompanied by a higher reflection coefficient of the MPP.

The use of a MPP alone could thus prove a low-frequency compromise displaying moderate absorption, acceptable reflection and good transmission loss.

3.3.2. Transmissibility and absorption of a MPP coupled to a solid plate

Transmission loss and reflection coefficient are shown on next 3 figures for the cases of normal incidence (Figure 9), 45° oblique incidence (Figure 10) and diffuse field (Figure 11). The diffuse case was computed by integrating the solution for oblique incidence over all angles. Each figure

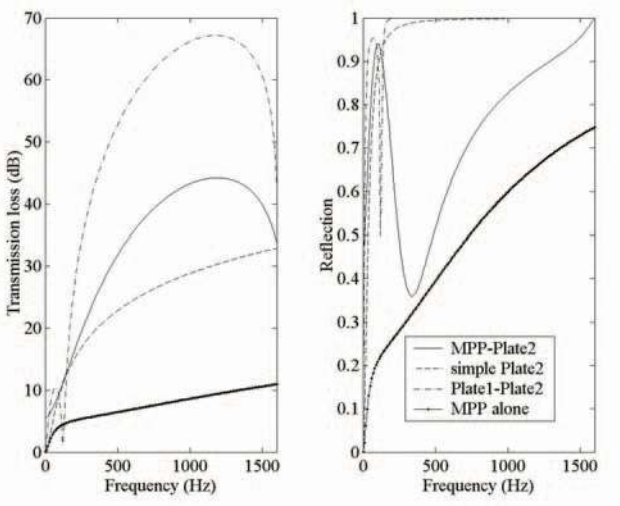

Figure 10. Transmission loss (left) and reflection coefficient (right) computed for 45° oblique incidence. The curves represent the basic system (MPP + solid plate), simple plate alone, two simple plates and MPP alone. The MPP's is made of steel, hole diameter 0.5 mm, thickness 1 mm, perforation ratio 0.55%. The steel solid plate is 0.7 mm thick. The air gap is 0.15 m.

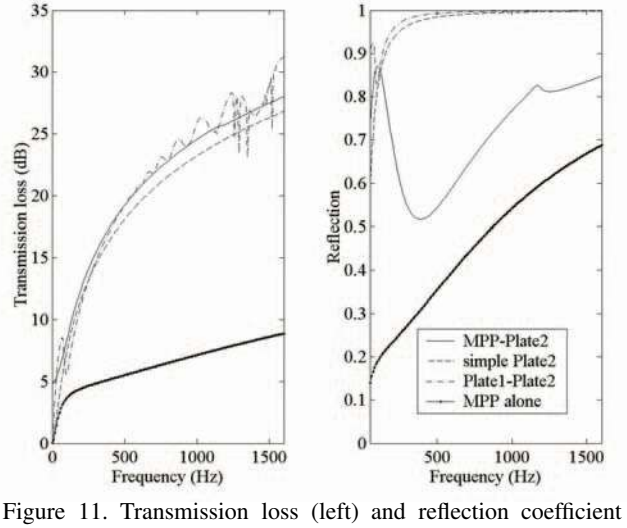

Figure 11. Transmission loss (left) and reflection coefficient (right) computed for diffuse field conditions. The curves represent the basic system (MPP + solid plate), simple plate alone, two simple plates and MPP alone. The MPP's is made of steel, hole diameter 0.5 mm, thickness 1 mm, perforation ratio 0.55%. The steel solid plate is 0.7 mm thick. The air gap is 0.15 m.

contains four curves, representing the basic MPP - simple plate system, the simple plate alone, two simple plates and the MPP alone. The case of the single simple plate is shown for the sake of comparison. Only the first and the fourth systems absorb energy; the damping effect of the second and third systems is negligible except at plate resonance.

One can notice that the difference between the transmission loss of MPP coupled to a simple plate (first case) and two simple plates (third case) can be as large as 28 dB. The latter shows an appreciable transmission loss, but in the absence of absorption the reflection is high, except at very low frequencies and near plate resonance. On the contrary, the MPP – simple plate system shows variation in reflection between 0 and 1 throughout the frequency range considered. The transmission loss of this system varies with frequency similar to the double plate system due to cavity effects. One can observe a difference in the frequencies of minimum transmission loss between these two cases, around 1200 Hz. In this state the plate boundary conditions of the two systems are different, so the acoustic pressure and velocity in the air space are dissimilar, which changes the transmission loss extremes.

An average difference in transmission loss of 10 dB between the first system and the single plate is seen at frequencies below 1600 Hz. The maximum difference does not match maximum dissipation. Close to frequencies where the wavelength is $\lambda = 2d/n$, the MPP absorption is at minimum, and the transmission loss of the composed system is smaller than the transmission loss of the plate alone. Although the viscous effect is almost zero, the pressure fields in the inter-plate air gap is modified resulting in a change of excitation of the second plate. In the vicinity of this frequency the sound velocity is zero on the MPP, and the MPP absorption is zero too.

As the frequency rises, the transmission loss difference between the first system and the single plate increases. At 4000 Hz the transmission loss difference in normal incidence exceeds 25 dB. Figures 9, 10 and 11 show that the reflection of MPP alone increases with frequency. At high frequencies there is a screen effect which induces high reflection for the MPP composed system. And as the frequencies increases, the absorption peaks become narrower. At high frequencies, except at those producing the wavelengths of $\lambda = 4d/(2n+1)$, reflection and transmission dominate the absorption, thus the increase in transmission loss with frequency.

It can be seen that the transmission loss of the MPP alone is added to the transmission loss of the second plate alone, on which the cavity resonance effect is superimposed at frequencies where $\lambda = 4d/(2n+1)$.

3.3.3. Transmission and absorption of a MPP coupled to a thick plate

If the thickness of the solid plate is increased sufficiently, the coincidence frequency at oblique incidence will decrease below 1600 Hz, i.e. will enter the frequency range considered. At this frequency the transmission loss will become very small. Using a MPP in this case could improve the isolation due to the added absorption of the MPP.

On Figure 12 a very low transmission loss of only 20 dB is seen at the coincidence frequency. The loss increases by 12 dB if the MPP is used instead. Using an MPP reduces the coincidence effect without adding any porous materials.

If the second plate is thick enough the transmission tends toward zero. The second plate then acts as a rigid wall in normal incidence. The transmission and reflection are here exactly the same as in the case of normal propagation analysed in the first part.

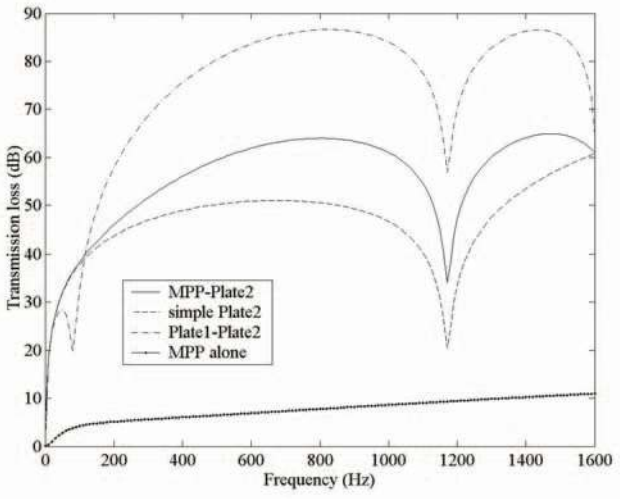

Figure 12. Transmission loss at 45° oblique incidence – MPP + thick solid plate of 20 mm thickness. The curves represent the basic system (MPP + solid plate), simple plate alone, two simple plates and MPP alone. The MPP is made of steel, hole diameter 0.5 mm, thickness 1 mm, perforation ratio 0.55%. The steel solid plate is 0.7 mm thick. The air gap is 0.15 m.

3.3.4. Analysis of reverse system

An analysis of a reverse system, equivalent to the one analysed so far, has been carried out in order to get additional insight in the behaviour of MPP / simple plate systems. The impedances of the two plates have been simply inversed in the model. Although a MPP plate system does not show reflection and absorption reciprocity, the transmission loss was found here to be perfectly reciprocal. The reverse system shows very high reflection (the reflection coefficient tends very quickly toward 1, exactly like the one of a single plate) which results in a very low pressure in the air gap and a poor MPP absorption. Because of very high reflection, the reverse configuration has lost all of the MPP advantages. Thus, when using a MPP, it has to be placed on the side of the acoustic source.

Probably the best solution would be to put one MPP on each side of a simple plate. Each MPP can then be given different characteristics (perforations, thickness, air gap distance) for an optimum effect.

4. Experimental results

In order to validate the 2-dimensional sound transmission model of the MPP system discussed, a few laboratory measurements have been carried out in diffuse field conditions.

4.1. Experimental set up

A large, 411 m^3 reverberant chamber of unparallel concrete walls was used for creating a diffuse sound field. The limiting frequency of the chamber, [22]

$$f_{lim} = \frac{c}{\sqrt[3]{4\pi\eta V}}, \quad \eta - \text{damping in air}, \tag{20}$$

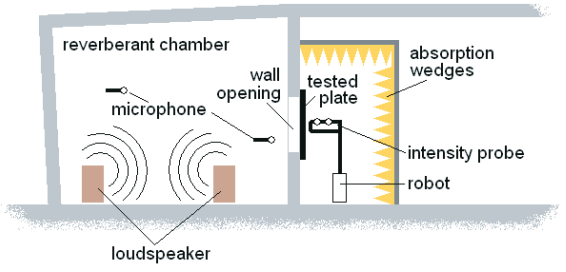

Figure 13. Experimental set-up for measurement of sound transmission in diffuse field.

was sufficiently low, ≈75–85 Hz, to allow for wide band measurements. The sound excitation was provided by two loudspeakers fed by random wideband noise. The electrical signals from the generator to the loudspeaker amplifiers was frequency equalized by 1/3 octave band equalizers to achieve a sound in the chamber as close to white noise as possible. The SPL in the reverberant chamber was 100–102 dB during measurements.

An anechoic cavity was connected externally to one of the walls of the reverberant chamber. Its role was to serve as a free-field reception space. The wall separating the two spaces was equipped with a rectangular opening 1.5×0.96 m into which the MPP system was installed, Figure 13.

The objective was to measure the transmission and absorption of the MPP system. This implied that the intensities at the two sides of the system had to be measured.

The normal component of intensity in a diffuse sound field is given by [22]:

$$I_{inc} = \frac{\langle p^2 \rangle}{4\rho_0 c}, \tag{21}$$

with the brackets indicating spatial average. Two microphones were placed in the reverberant chamber, which is considered to be sufficient to estimate the mean pressure square level.

Transmitted intensity was measured directly using a 2-microphone intensity probe (B&K type 2682) equipped with a 12mm spacer. Phase calibration of the microphone pair was done prior to measurements using a twin calibration cavity. Data acquisition was done using a 4-channel acquisition unit Oros 24.

In the measurement, the probe was oriented in the direction perpendicular to the wall opening at a distance of approx. 6 cm from the tested plate.

Measurement of reflected intensity in the reverberation chamber was performed by carrying out both intensity and sound pressure measurements. It is well known that intensity measurements in a reverberant field are particularly delicate. In order to obtain reliable results, frequency averaging in bands wider than 100 Hz was needed. The intensity was measured in close proximity to the tested system.

As the intensity probe could provide only the net intensity readings, the reflected intensity was obtained via:

$$I_{\text{reflected}} = I_{\text{incident}} - I_{\text{measured}}. \tag{22}$$

The measurement was done in about twenty points randomly selected in the middle region of the tested system. The results were then space averaged.

Two systems were tested:

- Reference system: 1.5 mm sheet made of Dural.
- MPP system: MPP (produced by Sontech) coupled to the Dural plate via a 30 cm deep cavity.

The MPP plate was bolted to the steel frame of the opening. An adhesive tape was placed around the circumference to avoid sound leakage.

The critical frequency of the plate, i.e. the frequency at which the plate flexural wave speed matches the sound speed is, [22]:

$$f_c = \frac{c^2}{2\pi t_{sp}} \sqrt{\frac{12\rho_{sp}(1-\nu^2)}{E}}. \tag{23}$$

The critical frequency of the Dural plate was at $\approx 7,9$ kHz. At frequencies below the critical one the plate will globally follow the mass law. The transmission loss rises thus with frequency by 6 dB per octave. In a diffuse field the loss is [22]:

$$R_{diff} = R_0 - 10\log_{10}(0.23R_0), \tag{24a}$$

with R_0 being the loss at normal incidence:

$$R_0 = 20\log_{10}\frac{\omega t_{sp}\rho_{sp}}{2\rho_0 c}. \tag{24b}$$

The preceding expressions concern an infinite plate. The tested plate was fairly large so it was expected that the middle section would behave on average as an infinite plate. It was found that statistically stable results were obtained already by doing measurements at 10 randomly spaced points located in the central zone. In order to improve stability of results, measurements were finally carried out in 25 points using 200 spectrum averages per point. The transmission loss was found by dividing the transmitted averaged intensity by incident averaged intensity.

A detailed analysis of the influence of boundary conditions on measurement results was done. The plate was excited by hammer impulses, the response was measured by a laser vibrometer. By comparing the resonant frequencies identified by measurements and separately computed it was found that the true boundary conditions were very close to clamped conditions. The marked modal behaviour of the plate was found to exist only at low frequencies. With the rise of frequency the plate response became increasingly similar to that of an infinite plate.

4.2. Analysis of results

In order to produce realistic simulation results, the transmission model had to be adapted to measurement conditions, [21]. In reality the sound waves do not impinge the plate at all angles of incidence. In particular, the grazing incidence could not take place; the wall opening of 30 cm depth certainly creates a strong screening effect on waves arriving at large incidence angles. Consequently the integration in the computation of diffuse field transmissibility was carried out for angles between 0 and an upper limiting angle smaller than 90°. This angle, 72°, was found by tuning the results obtained on the simple plate to the computation results.

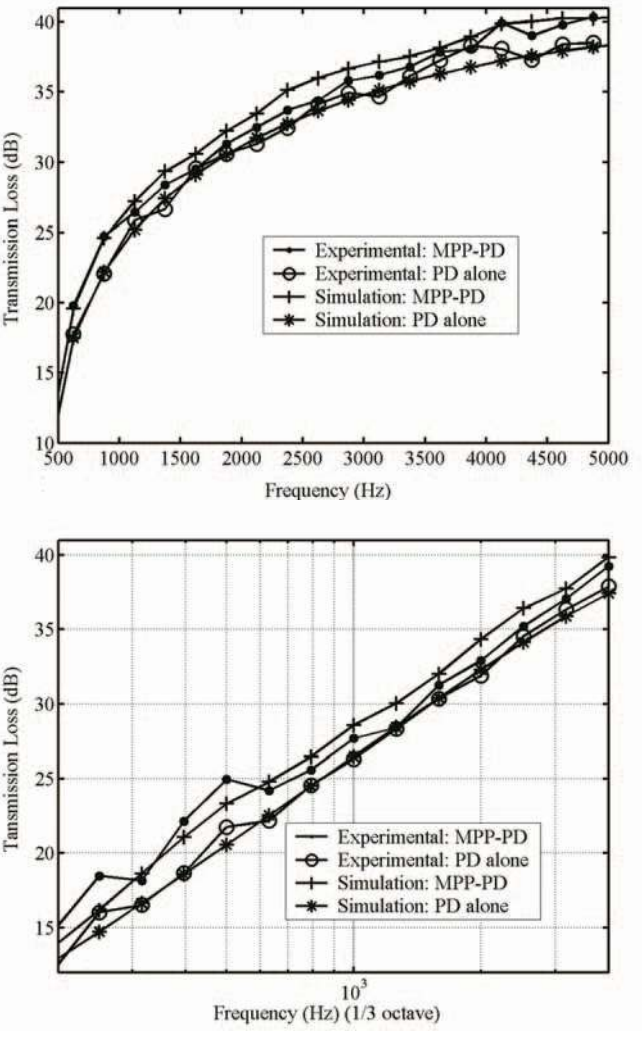

Figure 14. Transmission loss: measured and computed. MPP coupled to a simple Dural plate via a 30 cm air gap. a) constant 250 Hz band averaging b) 1/3 octave averaging.

The matching of the results, Figure 14, is fairly good except in the zone between 3,5 and 4,5 kHz. The computed transmission loss difference of the two systems, i.e. MPP + simple plate vs simple plate alone, is virtually the same as the measured difference at frequencies below 900 Hz and above 4,2 kHz. At intermediate frequencies the measured difference is slightly lower than the computed one, 1.5 dB at most.

Below 200 Hz, the measurement results were too unreliable to be taken into account.

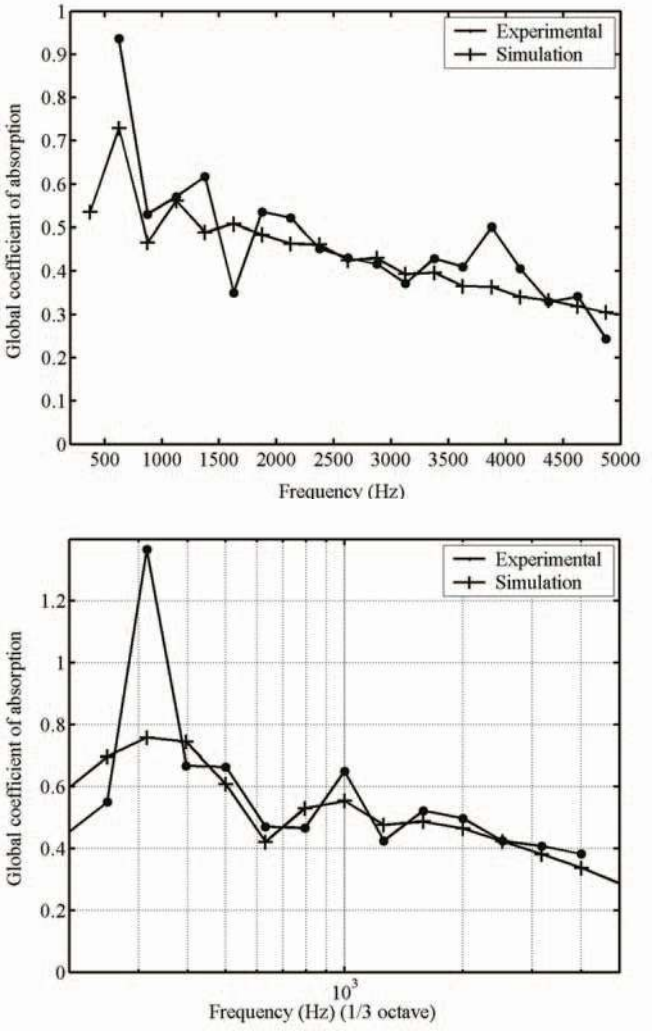

Figure 15. Global coefficient of absorption measured and computed. MPP coupled to a simple Dural plate via a 30 cm air gap. a) constant 250 Hz band averaging b) 1/3 octave averaging.

The global absorption as seen by the incident surface is:

$$\alpha_{glob} = 1 - \frac{I_{\text{reflected}}}{I_{\text{incident}}}. \tag{25}$$

The results seem to be globally correct. The matching between measurements and computation is good above 500 Hz. Below this frequency the matching is poor due to problems of intensity measurement and increase of statistical uncertainties.

5. Conclusions

A micro-perforated plate followed by a cavity closed by a rigid wall exhibits some interesting acoustical properties as found earlier by Maa. Its presence leads to non-negligible system absorption without the need to add any classical absorption material.

When backed by a lightweight simple panel, the acoustic properties of a micro-perforated plate can be further modified to produce interesting effects suitable for noise control. In summary, a MPP system increases the transmission loss, reduces reflections and weakens the coincidence effect.

The developed MPP system model has been validated by measurements. It can provide means of predicting the noise control performance of built-up MPP systems. Use of such systems in real applications could be a viable solution to the low frequency sound transmission problems.

Appendix

The next matrix represents the solution to the pressure amplitude within the system which is presented in Section 3: a MPP coupled via an air gap to a solid plate in oblique incidence.

$$\begin{pmatrix} -1 & 1 & 1 & \cdots \\ \left[1 - \frac{Z_{mpp}\cos\theta}{\rho_0 c}\right] & \left[1 - \frac{Z_{mpp}\cos\theta}{\rho_0 c}\right] & -1 & \\ 0 & 0 & \left[-\frac{1}{\rho_0 c}\right] & \\ 0 & 0 & -\mathrm{e}^{-\mathrm{j}kd\cos\theta} & \\ 0 & 0 & 0 & \end{pmatrix}$$

$$\begin{pmatrix} -1 & 0 & 0 \\ -1 & 0 & 0 \\ \cdots \left[\frac{\mathrm{e}^{-2\mathrm{j}kd\cos\theta}}{\rho_0 c}\right] & \left[-\frac{1}{\rho_0 c}\right] & 0 \\ -\mathrm{e}^{-\mathrm{j}kd\cos\theta} & -\mathrm{e}^{-\mathrm{j}kd\cos\theta} & Z_{sp} \\ 0 & \left[\frac{\mathrm{e}^{-\mathrm{j}kd\cos\theta}\cos\theta}{\rho_0 c\omega}\right] & \mathrm{j}\omega \end{pmatrix} \begin{pmatrix} A \\ B \\ C \\ D \\ E \\ F \end{pmatrix} = 0$$

References

[1] H. Reissner: Transmission of a normal and oblique-incidence plane compressional wave incident from a fluid on a solid plane parallel plate (in German). Helvetia Physica Acta **11** (1938) 140–145.

[2] A. Schoch, K. Feher: The mechanism of sound transmission through single leaf partitions. Acoustica **22** (1950) 270–275.

[3] H. Fescbach: Transmission loss of infinite single plates for random incidence. Report TIR 1, Bolt Beranek and Newman, 1954.

[4] A. London: Transmission of reverberant sound through double walls. J. Acoust. Soc. Am. **22** (1950) 270–277.

[5] G. Kurtze, B. G. Watters: New wall design for high transmission loss or high damping. J. Acoust. Soc. Am. **31** (1959) 739–748.

[6] M. Heckl: Investigation of orthotropic plates (in German). Acustica **10** (1960) 109–115.

[7] M. Heckl: Sound transmission loss of homogeneous single wall of finite size (in German). Acustica **10** (1960) 109–115.

[8] K. Goesele, U. Goesele: Influence of cavity damping on the air layer stiffness in double walls (in German). Acustica **38** (1977) 159–166.

[9] L. Feng, A. Nilsson: A new design of lightweight panel to improve static strength and sound isolation. Proceedings of Internoise-2000, Nice, France, 2000, 2455–2458.

[10] A. C. Nilsson: Wave propagation in and sound transmission through sandwich plates. J. Sound Vib. **138** (1990) 73–94.

[11] D. Y. Maa: Theory and design of microperforated panel sound-absorbing constructions. Scientia Sinica **18** (1975) 55–71.

[12] D. Y. Maa: Wide-band sound absorber based on microperforated panels. Chinese journal of acoustics **4** (1985) 197–108.

[13] D. Y. Maa: Potential of microperforated panel absorber. J. Acoust. Soc. Am. **104** (1998) 2861.

[14] J. Kang, H. V. Fuchs: Predicting the absorption of open weave textiles and microperforated membranes backed by an air space. J. Sound Vib. **220** (1999) 905–920.

[15] H. V. Fuchs, X. Zha: Acrylic-glass sound absorbers in the plenum of Deutscher Bundestag. Applied Acoustics **51** (1997) 211–217.

[16] Z. M. Zhang, X. T. Gu: The theoretical and application study on a double layer microperforated sound absorption structure. Acoustics letters **215** (1998) 399.

[17] B. Zhang, S. Lang, P. Ge, W. Zhuang: The study of sound absorption characteristic of micro-perforated panel with different diameter holes. Proceedings of Internoise-2000, Nice, France, 2000, 3871–3874.

[18] T. Dupont, G. Pavic, G. Laulagnet: Absorption and transmissibility of coupled microperforated plates. Proceeding of 17 th International Congress on Acoustics. Session Measurement techniques in structural acoustics, 2001, 34.

[19] I. B. Crandall: Theory of vibrating systems and sound. Ed. Van Nostran, 1926. 229.

[20] T. H. Melling: The acoustic impedance of perforates at medium and high sound pressure levels. J. Sound Vibr. **29** (1973) 1.

[21] M. Bruneau: Manual of acoustic fundamentals (in French). Hermes, 1998.

[22] C. Lesueur: Rayonnement acoustique des structures, vibroacoustique, intéractions fluide structure (in French). Editions Eyrolles, 1988.